

A ONCE-MOLTEN, COARSE-GRAINED, Ca-RICH INCLUSION IN ALLENDE

GLENN J. MacPHERSON¹ and LAWRENCE GROSSMAN^{1,2}

¹ *Department of Geophysical Sciences, University of Chicago, Chicago, IL 60637 (U.S.A.)*

² *Enrico Fermi Institute, University of Chicago, Chicago, IL 60637 (U.S.A.)*

Received June 2, 1980

Revised version received August 12, 1980

A compact, spheroidal Type B inclusion in Allende contains melilite laths that project radially inward from the inclusion edge which show interference growth textures. The combined textural and chemical features of this object cannot be explained by independent vapor-solid condensation of grains in space, followed by random aggregation of these grains into an inclusion. Rather, it probably formed from a once-molten droplet that crystallized in response to radiative cooling from its outer surface. The crystallization sequence in this and another similar inclusion in which oxygen isotopes have been measured is melilite-spinel-anorthite-fassaite. This sequence supports the idea that oxygen isotopic heterogeneities in coarse-grained inclusions were formed after complete solidification of these objects by partial exchange with a less ¹⁶O-rich gas, and not during or before a melting event.

1 Introduction

Coarse-grained, calcium-aluminum-rich inclusions [1] in Allende and other carbonaceous chondrites have been identified with the highest-temperature condensates predicted to have formed in the solar nebula [2]. Published petrographic evidence regarding the origin of these objects is ambiguous, however, and the community studying them is therefore split over the issue of whether they are truly the primitive vapor-to-solid condensates [3–5] or whether they passed through a molten stage either during or after condensation [6–10]. Grossman [11] suggested that there are both melted and unmelted types of these inclusions and we present here what we believe to be the most convincing evidence given to date that some of these inclusions were indeed molten.

Most arguments that coarse-grained inclusions were once molten are based on the spheroidal shapes [6,7] and compact textures [6] of many of these objects. Blander and Fuchs [6] described six inclusions from Allende and interpreted all of them in terms of crystallization from liquids. Their evidence for such an interpretation is of two kinds. (1) mineral

crystallization sequences deduced from textures in these inclusions are not in accord with predicted vapor-solid condensation sequences, e.g. refractory phases such as hibonite and perovskite are predicted to condense prior to melilite and spinel, yet these phases occur at the margins of some inclusions, (2) some of the inclusions have tight-fitting, poikilitic, ophitic, or allegedly eutectic textures that are supposedly characteristic of a liquid origin. In some of these inclusions, no sequence of crystallization could be determined from the textures.

In the first argument, it is assumed that vapor-solid condensation sequences are precisely known, which is not the case. For example, the condensation temperature of fassaite, a major phase in Type B inclusions, is not known relative to those of melilite and spinel. It is also assumed that, in a direct vapor-solid condensation process, phases accrete in the same order in which they condense. This assumption is not required and is discussed below. The second argument is unjustified: the textures described by Blander and Fuchs [6] can just as well be produced by metamorphism as by liquid crystallization. It has never been shown that tight-fitting or poikilitic textures could

not be produced by vapor-solid condensation. For example, one can envision that such a texture could result from condensation of fassate in a cloud densely packed with spinel. Also, liquid crystallization is generally expected to produce a well-defined sequence of crystallization except in the very fortuitous case where the liquid is eutectic or near-eutectic in bulk composition. Terrestrial igneous rocks usually show such a sequence. Blander and Fuchs' [6] inability to determine crystallization sequences in their coarse-grained inclusions might argue just as strongly for a metamorphic as for an igneous origin.

Kurat et al. [8] proposed supporting evidence by reporting an inclusion in Bali in which refractory element contents of melilite and pyroxene grains near the margin of the inclusion are higher than those of grains of the same phases in the core, while more volatile elements are enriched in the core grains relative to those in the margin. Kurat et al. [8] expected that inclusions formed by direct condensation of solids from a gas would have grains in their cores that are richer in refractories than those in their margins. Because this is contrary to what was observed, these workers concluded that the inclusion did not form in this way, but formed instead by volatilization and condensation processes accompanying impact melting. This conclusion, however, is based on the assumption that the grains which formed true condensate inclusions should have accreted in the order in which they condensed from a monotonically-cooling gas in a closed system. But this assumption is an unnecessary restriction, as one can envision solid material moving into nebular regions with different pressures, temperatures and/or bulk compositions from that in which it formed. Such material could easily have acted as a substrate for nucleation of phases that should have condensed prior to it in its original formation location.

More recently, Lorin et al. [9] described an inclusion with ophitic textures similar to terrestrial igneous rocks, and concluded by analogy that their inclusion was also once molten. We see no reason, however, why such ophitic-textured inclusions could not be produced by vapor-to-solid condensation, in a manner analogous to that discussed above for poikilitic inclusions.

Our purpose here is to describe an inclusion whose textural features cannot be explained by direct con-

densation of solids from a vapor, nor by metamorphism, but are completely consistent with a molten origin.

2. Analytical techniques

A highly compact inclusion with very little void space was discovered on a slab surface of the Allende meteorite and a polished thin section, TS33, was made of it and its surroundings. This was examined optically and also with a JEOL JSM35 scanning electron microscope equipped with a KEVEX Si(Li) X-ray detector. Mineral analyses were obtained by wavelength-dispersive methods with an ARL-EMX-SM, 3-spectrometer, automated electron microprobe, operated at 15 keV accelerating voltage and 0.5 μ A beam current. Beam spot size was approximately 2 μ m. Natural and synthetic minerals and glasses were used as standards. Data were reduced via an on-line NOVA 2/10 computer, using the program MAGIC (J. W. Colby, Bell Laboratories) for matrix corrections.

3 Description

The inclusion, labelled TS33F1 in thin section, is a white, 1.1 cm diameter sphere. A photomicrograph is shown in Fig. 1. The most distinctive features are the elongate ($L/W \leq 10:1$) melilite laths *each of which terminates at and projects inward from the inclusion rim*. These melilites are up to 5 mm in length and the smallest crystals are confined to the inclusion margin, while the fewer long crystals project all the way into the core. All are strongly shocked, with kink-bands oriented perpendicular to the length of the crystals. Closer examination (Fig. 2) of the melilites near the inclusion margin shows that neighboring crystals abut against one another and, in many cases, short crystals terminate against the sides of neighboring long crystals. This kind of interference growth texture, displayed by crystals growing on a common surface, is similar to textures found in devitrified glass shards in terrestrial ash flow tuffs and is referred to as axiohtic texture [12]. All of the melilites in TS33F1 are optically zoned, with bright, first-order white or yellow birefringent cores

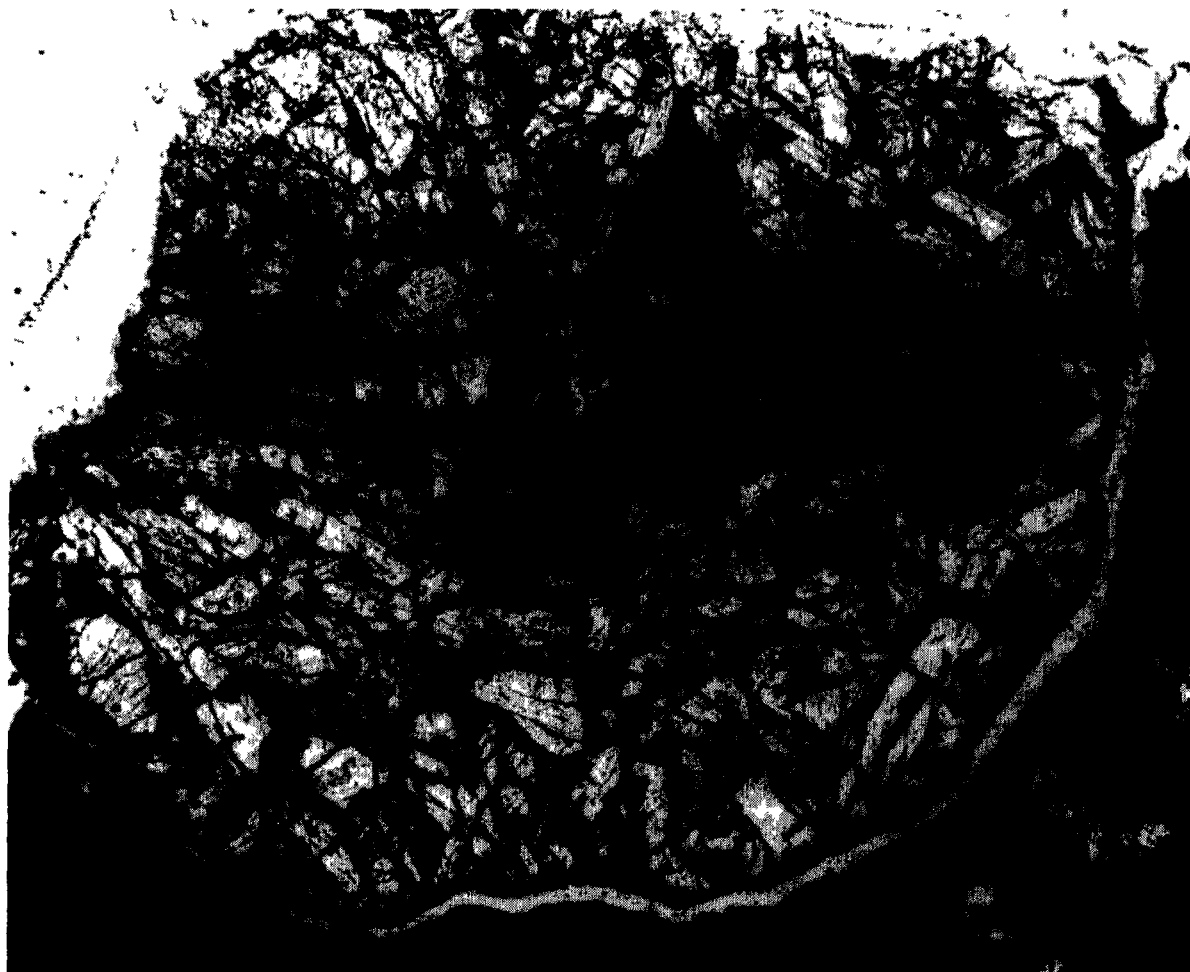
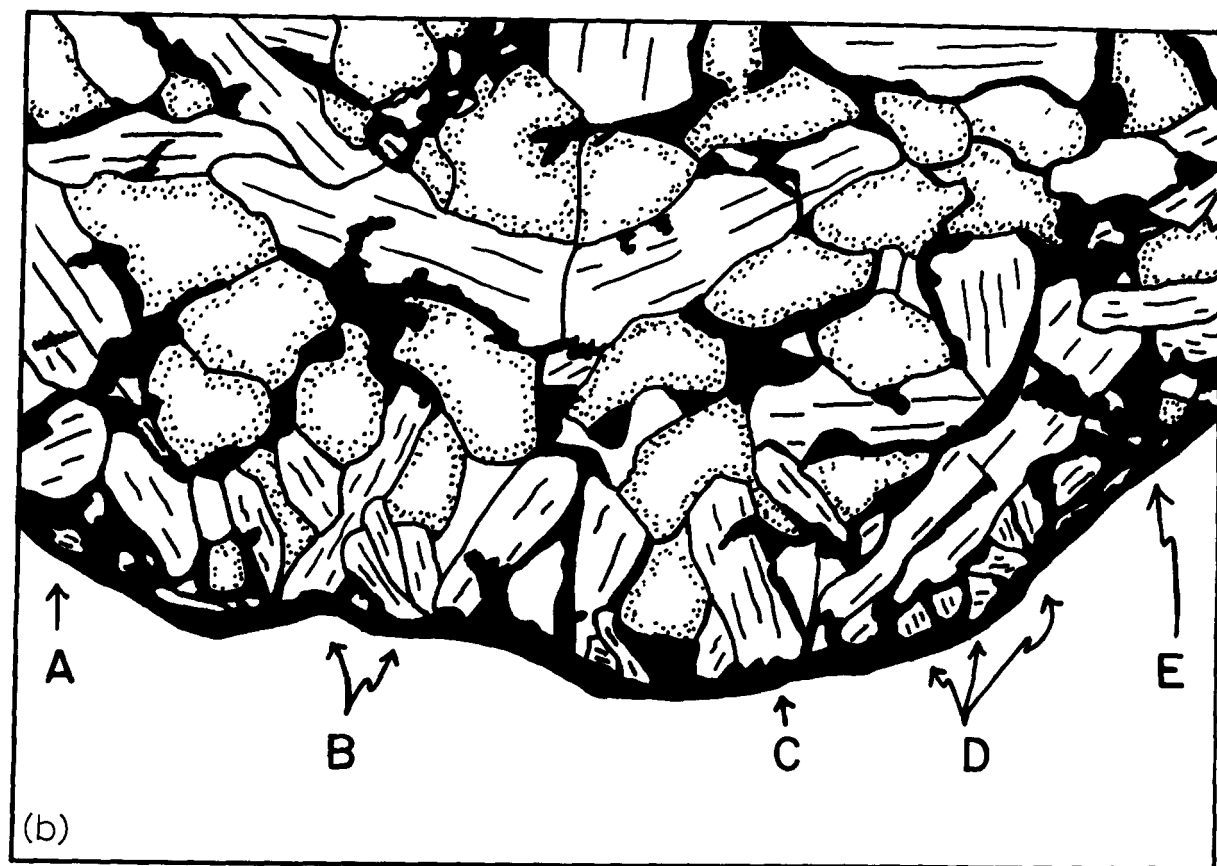
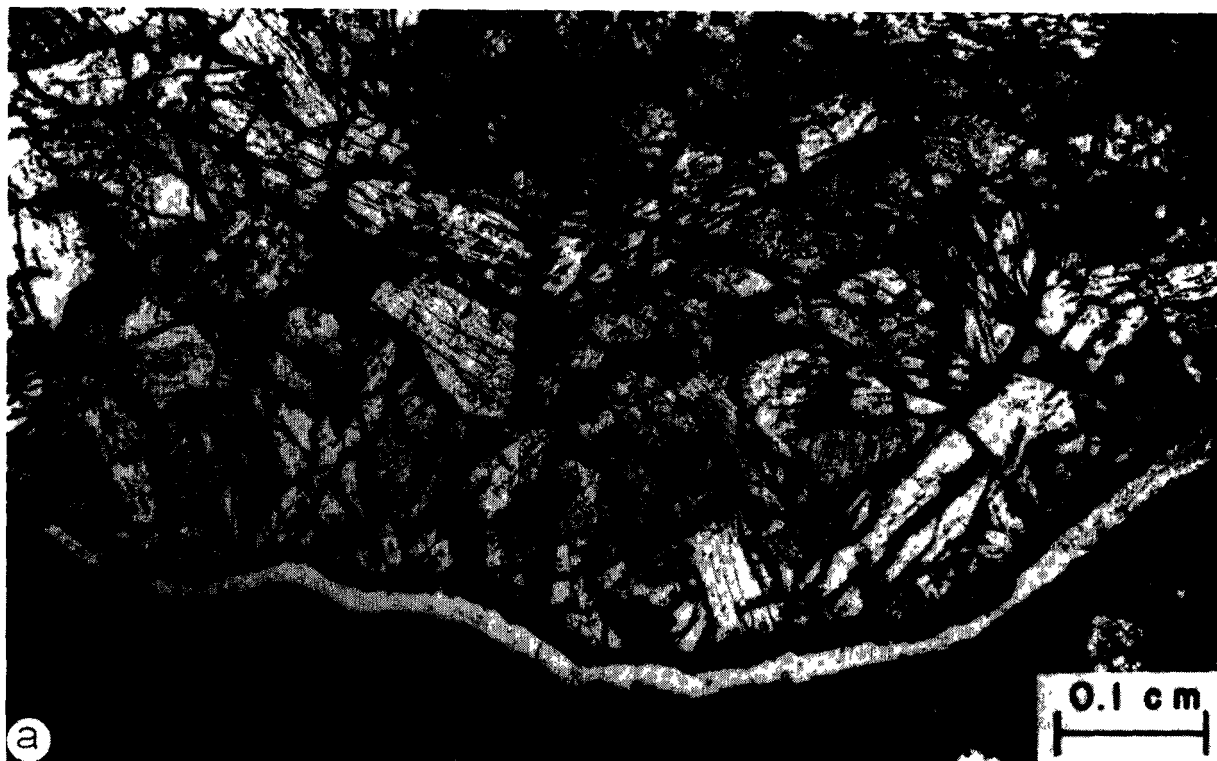


Fig 1 TS33F1, containing long melilite laths (white), anhedral fassaite (grey), sparse anorthites, and spinel as inclusions in all the above phases. The white "rim" is epoxy where the inclusion has separated from the dark Allende matrix during thin section preparation. Transmitted light, the inclusion is 1.1 cm in diameter.

and grey or anomalous-blue birefringent rims. These zoning patterns are directly correlated with compositional zoning (see section 4).

Subordinate to the melilites in both abundance and shape are grey-green pleochroic fassaite crystals. Fassaite is most abundant near the inclusion core,

Fig 2 (a) Enlarged photomicrograph of a portion of the margin in TS33F1. (b) Tracing of the photomicrograph in (a) showing melilite (cleavage traces parallel to length), fassaite (stippled), anorthite (clear), and alteration products (black). Scale same as in (a). (A) A short stubby melilite on the inclusion rim abuts against a long melilite lath that extends from the upper left edge of the drawing to the lower left margin of the inclusion. (B) Several narrow melilite laths extending in criss-cross fashion away from the inclusion margin. Two laths intersect each other and both are narrower at the region of intersection, suggesting mutual interference during width-wise growth of each crystal. (C) A euhedral melilite lath oriented nearly perpendicular to the inclusion margin has blocked the growth of a small melilite on the lower left of the big crystal. Note also the large fassaite crystal that envelops the euhedral termination of the large melilite, suggesting that the pyroxene grew after the melilite had formed. (D) A long melilite oriented at a small angle to the inclusion margin has obstructed the growth of several small melilites that abut against its lower side. (E) The end of the long melilite in (D) is abutting against the end of another, smaller melilite lath that extends horizontally from the right edge of the drawing.



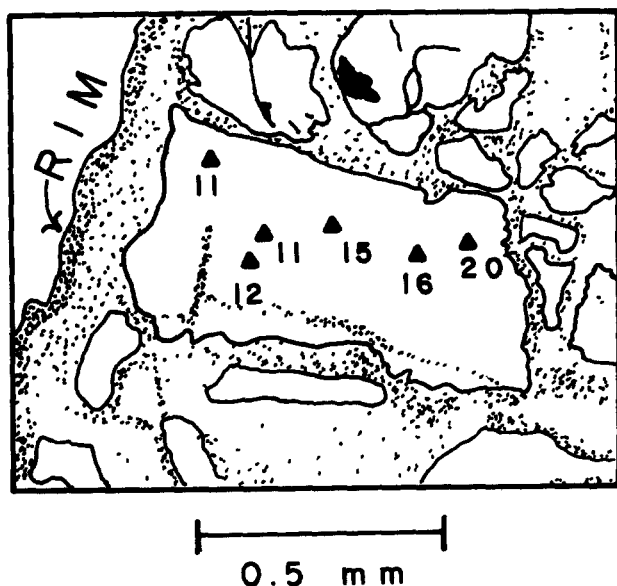


Fig 3 Åkermanite contents of the core of a single melilite crystal, as determined by electron microprobe analysis. The Åkermanite content increases along the length of the crystal, away from the margin of TS33F1

where it occurs as anhedral crystals. Fassaites near the inclusion rim either partially surround the euhedral melilites or fill angular interstitial voids between them. All of the fassaites are concentrically zoned, being somewhat more intensely colored in their cores. Some crystals have faintly visible sector zoning.

Anorthites are minor in abundance and occur as irregular to tabular crystals. No optical zonation is visible.

Spinel occurs as inclusions within all other phases, but are mostly concentrated toward the inclusion core. In melilite, the spinels occur mostly near crystal rims. Melilite crystals very near the margin of TS33F1 have virtually no spinel in their cores, suggesting that melilite began to crystallize slightly prior to spinel. Fassaites, in contrast, are densely crowded with spinel inclusions almost everywhere, suggesting that pyroxene began crystallizing long after spinel. Anorthites, in some cases, are nearly spinel-free, but elsewhere contain many spinel inclusions.

Fremdlinge [13] have not been found in this inclusion. Numerous tiny ($\leq 5 \mu\text{m}$) metal beads (mostly Ni-Fe) do occur as inclusions associated closely with spinel.

The rim sequence around TS33F1 is very thin and consists of pink spinel, tiny anorthite blades, grossular and nepheline. These phases also occur in the inclusion interior as alteration products along fractures and grain boundaries.

4 Mineral chemistry

The compositions of individual melilite crystals vary in two ways: (1) the crystals are concentrically zoned, and (2) crystals near and projecting inward from the inclusion margin change composition progressively along their length. All melilite shows normal concentric zoning, with aluminum-rich (gehlenitic) cores and magnesium-rich (åkermanitic) rims. Crystals near the inclusion margin range in composition from cores of $\text{Åk} \sim 10$ to rims of $\text{Åk} \sim 14$. Crystals near the core of TS33F1 have a much more extreme range, from cores of $\text{Åk} \sim 15$ to rims of $\text{Åk} \sim 60$. The second kind of melilite composition variation is shown in Fig 3. A single melilite lath, oriented approximately perpendicular to the inclusion margin, changes composition *along its length* from $\text{Åk} 11$ near the margin to $\text{Åk} 20$ toward the inclusion core. All of these analyses are from the core of the crystal, so this is not an effect of the normal core-rim zonation discussed above. Minor element contents of all melilites in TS33F1 are uniformly very low: $\text{FeO} \leq 0.07 \text{ wt } \%$, $\text{K}_2\text{O} < 0.02 \%$, $\text{Na}_2\text{O} \leq 0.02 \%$.

The fassaites in TS33F1 contain $\sim 19\text{--}22 \text{ wt } \%$ Al_2O_3 and $5\text{--}11 \%$ TiO_2 (calculated as Ti^{4+}). These components tend to be somewhat enriched in the crystal cores relative to the rims. Two electron microprobe analyses showing the ranges in composition are given in Table 1. No variation of pyroxene composition as a function of location within the inclusion was detected. Minor element contents in these pyroxenes are low and show little variation (Table 1).

Spinel is near end-member MgAl_2O_4 as shown in Table 1, with the exception only of pink spinels in the rim layers that are FeO-rich (up to $\sim 5.5 \%$). On average, V_2O_3 is slightly higher in spinels near the inclusion margin than spinels near the core. Also, spinels enclosed in melilite are slightly richer in V_2O_3 ($0.20\text{--}0.25 \%$) than spinels in fassaites ($0.10\text{--}0.25 \%$). Plagioclases show very little variation in composition and are uniformly $\text{An } 99.0\text{--}99.3$. The con-

TABLE 1

Electron microprobe analyses of phases in TS33F1

	1	2	3	4	5
	Fassaite	Fassaite	Fassaite (12*)	Spinel	Spinel (40*)
SiO ₂	42.68	35.15		—	—
Al ₂ O ₃	18.70	21.85		70.47	
TiO ₂	5.30	10.80		0.39	0.14–0.69
MgO	9.79	7.19		27.95	
FeO	n.d.	n.d.	n.d.	0.06	n.d. –0.16
CaO	25.03	25.54		—	—
Na ₂ O	n.d.	n.d.	n.d.	—	—
MnO	n.d.	n.d.	n.d.	—	—
NiO	n.d.	n.d.	n.d.	—	—
Cr ₂ O ₃	0.06	0.04	0.03–0.06	0.13	0.09–0.16
V ₂ O ₃	—	—	—	0.23	0.12–0.25
Total	101.56	100.60		99.23	

1 = most Ti-poor fassaite, 2 = most Ti-rich fassaite, 3 = ranges of minor element contents in fassaites, 4 = spinel from the interior of the inclusion, 5 = ranges of minor element contents in spinels

n.d. = not detected, — = not analyzed

* Number of analyses

centrations of FeO, K₂O and BaO are each less than 0.02 wt %. MgO contents are slightly lower in anorthites near the inclusion margin (0.13–0.14%) than in anorthites near the core (0.15–0.27%), in accord with similar results in other Type B inclusions [9,14]

5 Discussion

The melilite laths in the outer zone of TS33F1 all share one feature in common despite great variations in their lengths, one end of each crystal is located on the inclusion margin. The most logical interpretation is that the melilites all nucleated on the outer surface and grew inward from it. This interpretation is strongly supported by the fact that the other ends of the shortest melilite crystals abut against and terminate at the sides of neighboring longer crystals, implying that the long crystals hindered further growth of the short ones and that, therefore, the direction of growth was inward. The longest crystals are those that nucleated first and thus encountered no obstructions during growth. The fact that the melilites grew so close together that they

interfered with one another's growth cannot be explained by independent condensation of separate grains in space and subsequent random aggregation of them into an inclusion.

Experimentally determined phase equilibria [15] in the system gehlenite (Ca₂Al₂SiO₇)–åkermanite (Ca₂MgSi₂O₇) support the interpretation that the melilite laths did indeed grow inward. This system shows complete solid solution, with a minimum in the liquidus loop at Åk 72. On the aluminum-rich side of the minimum, both liquid and crystals become progressively enriched in magnesium with falling temperature and experiments [16] indicate that this is true even in the presence of additional components. Thus, rapidly-crystallized melilites will be zoned from gehlenite-rich cores to åkermanite-rich rims. The melilites in TS33F1 are concentrically zoned in just this manner and, in addition, individual laths become progressively enriched in magnesium along their lengths away from the inclusion margin. The highest temperature portions of these crystals are thus located at the inclusion margin, implying that the crystals began crystallizing there and grew inward with falling temperature.

Two hypotheses can be advanced to explain all of the above features (1) vapor condensation of crystals inside a hollow spherical shell, or (2) crystallization of a molten droplet. We cannot envisage how, in the first model, such a precursor shell might have formed to act as a substrate for subsequent vapor-solid condensation inside it, or how it later became filled in. On the other hand, the textures of TS33F1 are entirely consistent with crystallization of a free-floating liquid droplet in response to radiative cooling from its outer surface.

The textures in this inclusion could not have been produced by metamorphism. If this were the case, the euhedral melilite laths would have formed by solid-state diffusion of components toward the growing crystals. The problem is that no phase other than spinel occurs as inclusions in melilite. The other phases that had to break down to supply components to the growing melilites must have either reacted completely to form melilite only, or residual components diffused away from the melilites to form other phases, or residual solids were physically pushed aside as the melilites grew. The first case is highly unlikely. The second alternative requires that diffusion was rapid relative to crystallization times, in which case the melilite crystals should not be compositionally zoned as they now are. In the third case, since the melilites do contain inclusions of spinel, they were apparently unable to push aside all solid grains they encountered during growth. Since they contain only spinel, we conclude that the melilites grew in a medium in which spinel was the only other solid phase. A second difficulty with the metamorphism model is why melilite and *only* melilite, nucleated preferentially at the outer surface of the inclusion. Without a thermal gradient, this could only happen if the outer zone had a composition more favorable for the nucleation and growth of melilite than of other phases. In this case, melilite should be largely confined to the outer zone where the necessary components for growth were most readily available. Yet the melilites often extend far into the center of the inclusion, suggesting that any original compositional heterogeneity was slight. In terrestrial metamorphic rocks, many phases, especially aluminum silicates, are commonly confined largely to bands with a favorable composition.

6 Implications for oxygen isotope studies

The discovery by Clayton et al. [17] that spinels and fassaites are enriched in ^{16}O by as much as 5% relative to melilites within the same coarse-grained inclusion is difficult to reconcile with a molten origin for any of these objects. Two attempts to do so were based on the assumption that the crystallization sequence of all Type B inclusions was that determined by Seitz and Kushiro [18] in phase equilibrium studies of a composition that lies within the range of bulk compositions of coarse-grained inclusions. In that work, spinel and fassaite crystallized prior to melilite during cooling. In one attempt, Clayton et al. [17] proposed a model in which pre-solar, ^{16}O -rich spinel and perovskite grains were introduced into the more ^{17}O - and ^{18}O -rich solar nebula during its condensation and were mixed with lower-temperature solar nebular condensates to form precursors to the inclusions. Melting of all the solid phases except spinel occurred at an intermediate stage of condensation. Re-solidification of the liquid resulted in ^{16}O -rich spinels enclosed within more ^{17}O - and ^{18}O -rich melilites and fassaites. Clayton and his co-workers were unable to explain why the fassaites are also ^{16}O -rich. In another attempt [11], completely molten droplets were initially rich in ^{16}O . During crystallization, the droplets were immersed in a more ^{17}O - and ^{18}O -rich gas that attempted to equilibrate isotopically with the liquid. The first minerals to crystallize, spinel and fassaite, acquired the ^{16}O -rich signature of the original liquid. Melilite crystallized after significant isotopic equilibration had occurred and thus acquired more ^{17}O - and ^{18}O -rich compositions.

Both of the above models require that spinel crystallizes at much higher temperatures than melilite, so that the spinel either never melts or else crystallizes long before melilite during solidification. We infer, however, that melilite crystallized first in TS33F1, followed by spinel, anorthite and, finally, fassaite for the following reasons. The ends of melilite laths at the inclusion margin are spinel-free in their cores and, towards the inclusion interior, the melilite cores have fewer and smaller spinel inclusions than the melilite rims. We thus conclude that melilite began crystallizing before spinel. Anorthites have spinel inclusions even near the margin of TS33F1, and no relationship exists between the sizes of enclosed spinels or their

abundance and position within the anorthite crystals. Anorthite thus began crystallizing after spinel and therefore after melilite. Fassaite is everywhere choked with numerous spinel inclusions, more numerous than in either melilite or anorthite. Furthermore, fassaite crystal shapes are determined by the shapes of adjoining melilite laths. Fassaite was thus probably the last phase to nucleate.

One of the samples studied by Clayton et al. [17], A13S4, and illustrated in their fig. 4, is identical in almost every respect to TS33F1. Melilite was the first phase to crystallize in it, but is nonetheless depleted in ^{16}O relative to spinel and fassaite as in the case of all other inclusions studied by Clayton et al. [17]. The isotopic heterogeneity cannot, therefore, be explained by either the model of Clayton et al. [17], or the model of Grossman [11], since both of these models require spinel to crystallize before melilite. Rather, our evidence supports a model in which the ^{16}O -rich coarse-grained inclusions partially equilibrated *in the solid state* with a more ^{18}O -, ^{17}O -rich gas. This occurred after melting and complete crystallization of A13S4, perhaps during the same process that caused alteration to grossular, nepheline and other secondary phases. In this model, the isotopic compositions of the various phases are controlled by the differing rates of oxygen diffusion into these solids. Spinel has a dense structure and therefore a low oxygen diffusion coefficient relative to the more open-structured melilites, and the fassaite is intermediate in these properties between melilites and spinels. The model adopted here is like that of Blander and Fuchs [6] in that isotopic heterogeneity was produced by partial exchange after complete solidification following melting, but here the similarity ends. That model required the oxygen isotopic composition of the initial solids to be pure ^{16}O , while evidence reviewed in Grossman [11] suggests that they began at a $\delta^{17}\text{O}$ of $\sim 40\text{‰}$.

7 Conclusions

The textural and chemical features of TS33F1 cannot be explained by direct vapor-solid condensation, but suggest rather that this object solidified from a molten droplet. Melilite crystallized before spinel in TS33F1 and also in another, texturally similar inclusion in which the spinels are enriched in

^{16}O relative to the melilites [17]. This observation suggests that oxygen isotope heterogeneities in once-molten coarse-grained inclusions originated after complete solidification of these objects, and not during or before crystallization.

Acknowledgements

We thank R.N. Clayton, A.M. Davis, and I.D. Hutcheon for helpful discussions. M. Bowie typed the manuscript with great speed and accuracy. This research was supported by NASA grant NGR 14-001-249.

References

1. L. Grossman and R. Ganapathy, Volatile elements in Allende inclusions, *Proc. Lunar Sci. Conf.* 6 (1975) 1729–1736.
2. L. Grossman, Condensation in the primitive solar nebula, *Geochim. Cosmochim. Acta* 36 (1972) 597–619.
3. J.M. Allen, L. Grossman, A.M. Davis and I.D. Hutcheon, Mineralogy, textures and mode of formation of a hibonite-bearing Allende inclusion, *Proc. Lunar Planet. Sci. Conf.* 9 (1978) 1209–1233.
4. A. El Goresy, K. Nagel and P. Ramdohr, Spinel framboids and fremdlinge in Allende inclusions: possible sequential markers in the early history of the solar system, *Proc. Lunar Planet. Sci. Conf.* 10 (1979) 833–850.
5. S.E. Haggerty, The Allende meteorite: evidence for a new cosmo-thermometer based on $\text{Ti}^{3+}/\text{Ti}^{4+}$, *Nature* 276 (1978) 221–225.
6. M. Blander and L.H. Fuchs, Calcium-aluminum-rich inclusions in the Allende meteorite: evidence for a liquid origin, *Geochim. Cosmochim. Acta* 39 (1975) 1605–1619.
7. B. Mason, The Allende meteorite: cosmochemistry's Rosetta Stone?, *Accounts Chem. Res.* 8 (1975) 217–224.
8. G. Kurat, G. Hohnke and K. Fredriksson, Zoned Ca-Al-rich chondrule in Bali: new evidence against the primordial condensation model, *Earth Planet. Sci. Lett.* 26 (1975) 140–144.
9. J.C. Lonn, M.C. Michel-Lévy and C. Desnoyers, Ophitic Ca-Al inclusions in the Allende and Leoville meteorites: a petrographic and ion microprobe study, *Meteoritics* 13 (1978) 537–540 (abstract).
10. D.A. Wark, G.J. Wasserburg and J.F. Lovering, Structural features of some Allende coarse-grained Ca-Al-rich inclusions: chondrules within chondrules?, in *Lunar and Planetary Science X* (Lunar Science Institute, Houston, Texas, 1979) 1292–1294.

- 11 L Grossman, Refractory inclusions in the Allende meteorite, *Annu Rev Earth Planet Sci* 8 (1980) 559–608
- 12 C S Ross and R L Smith, Ash-flow tuffs their origin geologic relations and identification, *U S Geol Surv , Prof Paper* 366 (1961) 81 pp
- 13 A El Goresy, K Nagel and P Ramdohr, Fremdlinge and their noble relatives, *Proc Lunar Planet Sci Conf* 9 (1978) 1279–1303
- 14 I M Steele, J V Smith, I D Hutcheon and R N Clayton, Allende inclusions cathodoluminescence petrography anorthite and spinel chemistry Mg isotopes, in *Lunar and Planetary Science IX* (Lunar Science Institute, Houston, Texas, 1978) 1104–1106 (abstract)
- 15 E F Osborn and J F Schairer, The ternary system pseudowollastonite-åkermanite-gehlenite, *Am J Sci* 239 (1941) 715–763
- 16 K H Gee and E F Osborn, Phase equilibria at liquidus temperatures in a part of the system $\text{CaO-MgO-Al}_2\text{O}_3\text{-SiO}_2$ the system $\text{Ca}_2\text{MgSi}_2\text{O}_7\text{-Ca}_2\text{Al}_2\text{SiO}_7\text{-CaMgSi}_2\text{O}_6\text{-CaAl}_2\text{Si}_2\text{O}_8$, *Bull Earth Miner Sci , Exp Station Penn State Univ* 85 (1969) 23–51
- 17 R N Clayton, N Onuma, L Grossman and T.K Mayeda, Distribution of the pre-solar component in Allende and other carbonaceous chondrites, *Earth Planet Sci Lett* 34 (1977) 209–224
- 18 M G Seltz and I Kushiro, Melting relations of the Allende meteorite, *Science* 183 (1974) 954–957